Materials Research, Vol. 5, No. 3, 379-384, 2002.

Interaction Between Second-Phase Particle Dissolution and Abnormal Grain Growth in an Austenitic Stainless Steel

J.C. Dutra[a], F. Siciliano Jr.*[b] and A.F. Padilha[b]

[a]*Department of Metallurgy, Faculty of Industrial Engineering*
Av. Humberto de Alencar C. Branco, 3972, 09850-901 São Bernardo do Campo – SP, Brazil
[b]*Department of Metallurgical and Materials Engineering, University of São Paulo,*
Av. Prof. Mello Morais, 2463, 05508-900 São Paulo - SP, Brazil

Received: September, 27, 2001; Revised: July 10, 2002

The continuing development of stainless steels has resulted in complex steel compositions with substantial amounts of alloying elements. The benefits of such additions invariably come attached to unavoidable disadvantages. One of the most critical item is the potential microstructural instability of the material. Alloying elements may be in a supersaturated solid solution, in which the precipitation of carbides, nitrides, borides and intermetallic phases occurs in a wide range of temperatures. In order to dissolve the mentioned precipitates, solution annealing is commonly performed. However, at the temperature range in which this treatment is carried out, the onset of abnormal grain growth can occur. The interaction between the dissolution of these second-phase particles and the occurrence of abnormal grain growth is investigated in this work. This study also shows that the thermodynamics and the kinetics of dissolution of precipitates may be used to predict whether abnormal grain growth takes place.

Keywords: *abnormal grain growth, stainless steels, precipitates*.

1. Introduction

There are basically two modes of grain growth: normal and abnormal[1-5]. During normal grain growth, sometimes called "continuous grain growth", the distribution of grain sizes remains approximately constant and the grains increase their diameter continuously and gradually, displaying a monomodal grain size distribution. During abnormal grain growth or secondary recrystallization (sometimes called "discontinuous grain growth"), particular grains grow exaggeratedly. The mean size of the others remains constant and the grain size distribution becomes very inhomogeneous. In other words, secondary recrystallization requires that the normal grain growth be strongly impeded, with the exception of a few grains, which act as nuclei.

Abnormal grain growth has been reported predominantly in alloys containing particles. When specimens containing a considerable amount of dispersed particles is annealed at a temperature close to the solvus point, in which part of the second-phase is dissolved, very large grains are formed by discontinuous grain growth[2].

Solution annealing heat treatments are usually performed to dissolve precipitates. Precipitates such as carbides, nitrides, sulphides, borides and several types of intermetallic phases are often present in the microstructure of austenitic stainless steels. Nitrides and sulphides are very stable and are not able to be dissolved in the solid state. On the other hand, carbides like $M_{23}C_6$ and M_6C as well as intermetallic phases may dissolve completely, depending on both the annealing temperatures and times. Carbides of the MC type can be only partly dissolved at usual annealing temperatures. These particles play a major role in both the grain growth inhibition and onset of abnormal grain growth[6].

The aim of the present study is, therefore, to investigate the interaction between second phase particles dissolution and abnormal grain growth during solution annealing heat treatments in a titanium stabilised austenitic stainless steel.

2. Experimental

The material chosen for this study was a stainless steel DIN X 10 NiCrMoTiB 15 15, Werkstoff-Nr. 1.4970. The

*e-mail: jdutra@cci.fei.br

chemical composition (in wt.%) is the following: 0.09%C, 14.6%Cr, 15%Ni, 0.46%Si, 1.70%Mn, 0.003%P, 0.004%S, 0.013%Co, 1.25%Mo, 0.46%Ti, 0.07%Cu, 0.0045%B, <0.05%Nb and 0.01%N. Several 10.5 mm-diameter bars were obtained by swaging and solution treatment. 10 mm-height specimens were cut off and submitted to heat treatments at temperatures of 1090, 1110, 1130, 1150, 1200, 1250, and 1300 °C for 5, 10, 15, 20, 25, 60, 125, 625, 3125 min. Additional specimens were aged at the temperatures 600, 700, 800, and 900 °C for 1000 h to evaluate the effect of the type of second-phase particles on grain growth. After these ageing treatments, they were treated at the temperatures 1090, 1130, and 1300 °C for 0.5, 5, and 25 h to provoke abnormal grain growth.

The metallographic preparation was performed by using standard procedures, while the final polishing was done by using Minimet®, with a solution of colloidal silica of 0.25 μm, for 45 min. The electrolytical etching used was a solution of 70% vol. nitric acid and 30% vol. distilled water, under a tension of 0.75 V and current density of 50 mA for 15 min. This etchant[7] allows to reveal only the grain boundaries necessary to measure the grain size. This procedure does not reveal annealing twins, which is good when grain size measurements are involved.

Grain size measurements were conducted according to ASTM E-112-82. Twenty fields were measured for each specimen. When abnormal grain growth took place, the volumetric fraction of gross grains was measured by quantitative analysis.

The second-phase particles were extracted by dissolving the matrix with a Berzelius solution[8], followed by a vacuum filtration with a membrane filter with a porous size of 0.1 μm. The residues obtained with this technique were analysed by X-ray diffraction in a Guinier-Jagodzinski apparatus with a monochromatic radiation of $Cuk_{\alpha 1}$. This was done to identify the type, structure and lattice parameters of the second-phase particles[9].

3. Results and Discussion

At the ageing temperature of 600 °C, the precipitation of $M_{23}C_6$ took place at grain boundaries. At 900 °C, there was exclusively the precipitation of $(Ti_{0.92}Mo_{0.08})C$ in both the interior of grains and at their boundaries. At 700 and 800 °C there was the presence of both precipitates mentioned above. The average grain sizes of the samples treated at 1090 and 1130 °C for all periods of time were basically the same: 44.7 and 42.9 μm, respectively. These average grain sizes were measured for grains subjected to normal grain growth inhibition only. Such procedure could not be done for samples treated at 1300 °C because of their low level of heterogeneity. In fact these samples presented only normal grain growth.

The evolution of abnormal grain growth was quantified by measuring the volume fraction of gross grains, as can be seen in Fig. 1 and Table 1. This figure shows that the onset of abnormal grain growth occurs earlier in those samples aged at 600 °C for 1000 h at 1090 or 1130 °C.

The analysis of Fig. 1 shows clearly that there is a distinct behaviour for the samples aged at 600 °C for 1000 h from the other ones. This figure shows lines of iso-percentage of gross grains for several temperatures and times and different previous ageing treatments. For similar periods of time, the percentage of gross grains is always higher in samples previously aged at 600 °C as compared to other samples, which means that the presence of $M_{23}C_6$ particles has an enhancement effect on the onset of abnormal grain growth. The tendency in the other cases is, therefore, to retard the onset of abnormal grain growth. This may also be concluded from the results presented in Table 1.

The tendency for second-phase particles dissolution may be analysed by the solubility product. The solubility products were calculated by a linear regression of the logarithm of the weight concentrations of the respective elements in solid solution in austenite as a function of the inverse of the absolute temperature. Supposing that the particles are $(Ti_{0.92}Mo_{0.08})C$, the following equation can be obtained[10]:

$$\log[0.92.Ti][0.08.Mo].[C] = 5.397 - \frac{10766}{T} \qquad (1)$$

where Ti, Mo, and C represent the weight percentages of these elements and T, the absolute temperature.

Table 1. Volumetric percentage of gross grains of the annealed samples at 1090 and 1130 °C for various periods of time and different start conditions (solution treated or aged at different temperatures for 1000 h).

Start Condition	Time (h) - Temperature 1090 °C			
	0	**0.5**	**5**	**25**
Solution Treated	0	0	44.7	97.6
600 °C-1000 h	2.8	2.8	3.8	50.4
700 °C-1000 h	1.8	1.2	4.0	24.0
800 °C-1000 h	2.0	4.2	6.2	13.4
900 °C-1000 h	3.4	5.6	11.0	6.0
Start Condition	Temperature 1130 °C			
Solution Treated	0	27.0	65.4	91.6
600 °C-1000 h	2.8	40.6	75.0	93.0
700 °C-1000 h	1.8	15.6	20.0	77.4
800 °C-1000 h	2.0	56.4	59.6	76.4
900 °C-1000 h	3.4	66.0	69.0	89.0

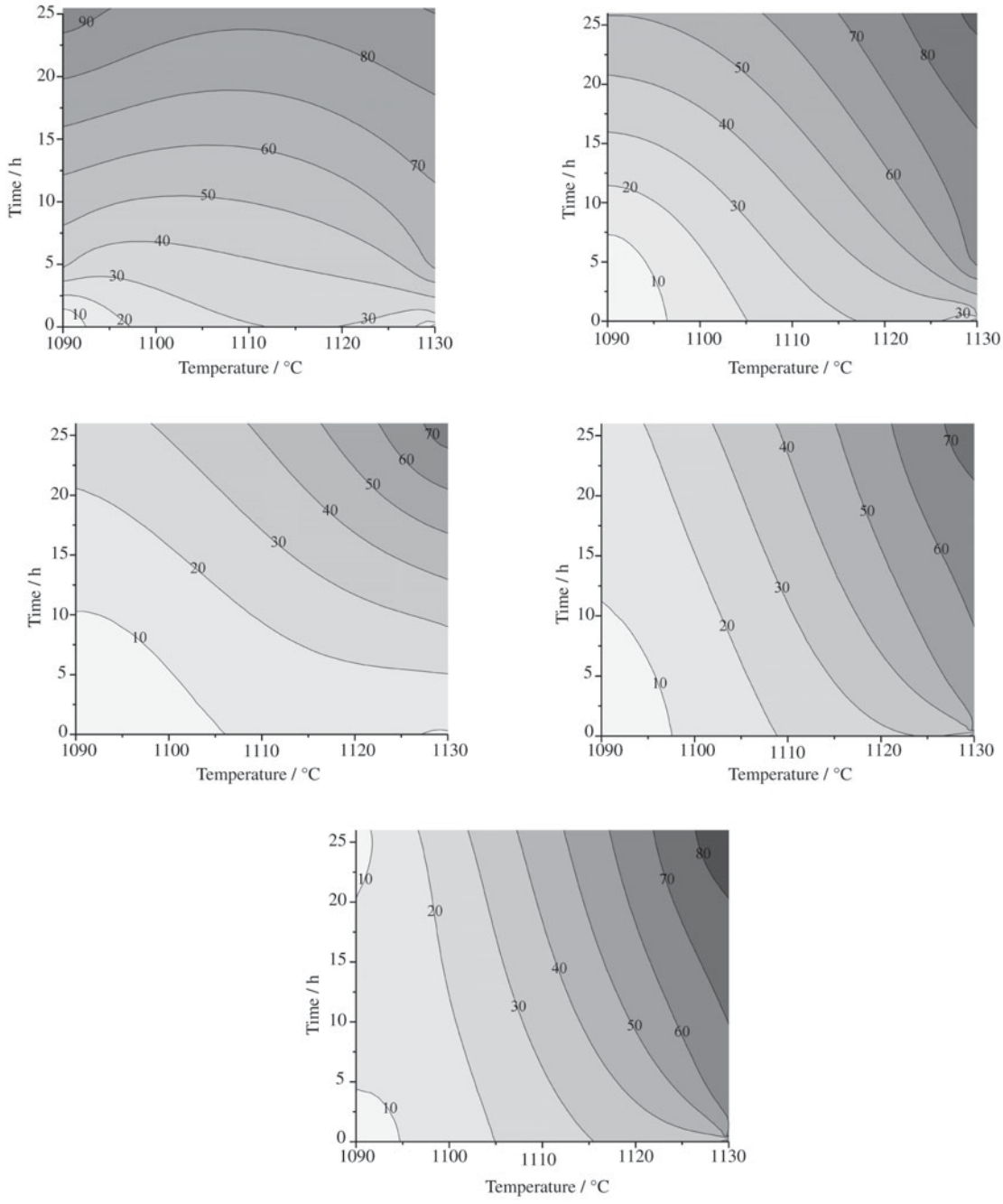

Figure 1. Evolution of the volumetric fraction of gross grains as a function of the annealing temperature and time for different start conditions. a) without start treatment (solution annealed); and ageing treatments for 1000 h at b) 600 °C; c) 700 °C; d) 800 °C; e) 900 °C.

The solubility product of $M_{23}C_6$ particles can be calculated by the following equation:

$$\log[C, ppm] = 7.771 - \frac{6272}{T} \quad (2)$$

It is worth mentioning that the latter solubility product was experimentally determined within the range 750 to 1100 °C[11].

As an example, the temperature in which all $M_{23}C_6$ particles may be in solid solution can be calculated, by sup-

posing that all the carbon contained in this steel is combined with Cr. Assuming this, the temperature obtained is 1029 °C. The same calculation for $(Ti_{0.92}Mo_{0.08})C$ particles gives an equilibrium temperature of 1169 °C, considering in this case that only half of the carbon is in solid solution in austenite. This temperature is higher than the one calculated for the $M_{23}C_6$ particles, which shows that $(Ti_{0.92}Mo_{0.08})C$ particles are more stable and, therefore, may only be completely dissolved in higher temperatures. This fact brings consequences to grain growth behaviour. Figure 1 shows the volumetric fraction of gross grains versus the type of second-phase particles and time for the annealing treatments at 1090 °C. It shows that abnormal grain growth occurs more extensively for the samples aged at 600 °C for 1000 h. These samples have predominantly $M_{23}C_6$ precipitated at grain boundaries. As these particles are less stable than $(Ti_{0.92}Mo_{0.08})C$ ones, although they impose grain growth inhibition in some regions, in others where dissolution takes place, abnormal grain growth may occur.

However, the kinetics of dissolution of these particles must also be analysed. Aaron and Kotler's model can be used to study this aspect[12-14]. The solution time can be calculated by the following equation:

$$t = \frac{r_0^2}{k.D_V} \tag{3}$$

where:

r_0 is the second-phase particle radius;

D_V is the volumetric diffusion coefficient;

k is the coefficient of supersaturation:

$$k = \frac{2(C_I - C_M)}{C_P - C_I} \tag{4}$$

where:

C_I is the concentration of solute atoms in equilibrium at the interface between matrix and particle at solution temperature T_S;

C_P is the concentration of solute atoms in equilibrium in the particle;

C_M is the concentration of solute atoms in equilibrium in the matrix at the solution temperature T_S.

By using the values of pre-exponential coefficient and the activation energy from the diffusion of chromium and titanium in austenite[15], it is possible to evaluate the time for the solution of the $M_{23}C_6$ and $(Ti_{0.92}Mo_{0.08})C$ particles, respectively, at various temperatures. The supersaturation coefficient of 0.1 is typical for common alloys[12]. The results of this analysis is shown in a graphical form in Fig. 2a, which presents a few curves showing the solution time for several $M_{23}C_6$ particles of different radii as a function of time and temperature. For instance, a 0.4 μm-diameter particle takes 10 s to reach complete dissolution at 1300 °C. Figure 2b, on the other hand, shows the dissolution curves of $(Ti_{0.92}Mo_{0.08})C$ particles of different radii at various temperatures.

The calculated times for dissolution of $M_{23}C_6$ and $(Ti_{0.92}Mo_{0.08})C$ particles can be seen in Table 2. The diameters considered are typical of the samples used in this work. This table shows that the times for dissolution of $M_{23}C_6$ precipitates are very short.

A comparison between the calculated dissolution times and the time for the onset of abnormal grain growth is seen

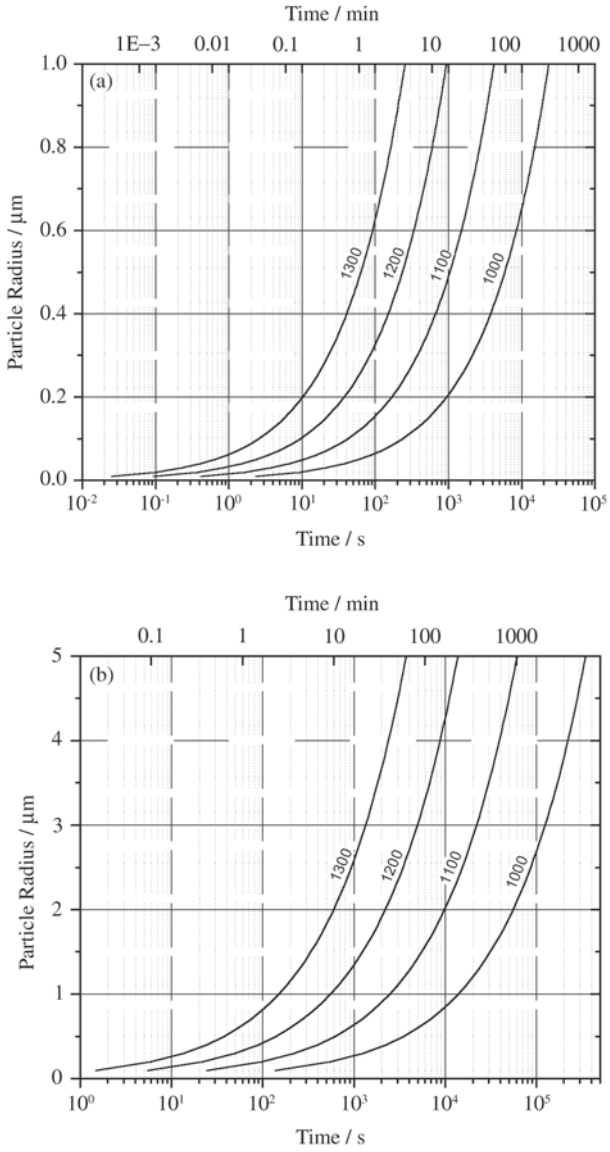

Figure 2. Curves showing the maximum radii of a) $M_{23}C_6$ particles and b) $(Ti_{0.92}Mo_{0.08})C$ particles, dissolved at time t, for various temperatures.

Table 2. Solution times (in seconds) calculated for $M_{23}C_6$ and $(Ti_{0.92}Mo_{0.08})C$ particles by using Aaron e Kotler's model. The diameters used in this calculation are typical of the samples of this work. For the $(Ti_{0.92}Mo_{0.08})C$ case, the times were obtained for the primary and secondary precipitates.

Type of particle	Diameter µm	1000 °C	1100 °C	1200 °C	1300 °C
$M_{23}C_6$	0.2	232.89	41.37	9.29	2.53
$M_{23}C_6$	0.4	931.59	165.47	37.16	10.09
$(Ti_{0.92}Mo_{0.08})C$ secondary ones	0.2	136.94	24.29	5.45	1.48
$(Ti_{0.92}Mo_{0.08})C$ primary ones	4.0	15.21 h	2.69 h	36.32 min	9.86 min

in Table 3. The average particle size considered for this analysis is 2.5 µm because it is the closest value to the analysed samples. This table shows that abnormal grain growth takes place in shorter times than the total dissolution of the particles. This analysis can be used to predict Fig. 3, which was produced after examining many samples treated at different times and temperatures. As a consequence of the partial dissolution of particles, some grain boundaries can be free for moving, and this effect leads to a preferential growth, which initiates abnormal grain growth.

4. Conclusions

The following conclusions can be drawn from this work:

- Within the temperature range of abnormal grain growth occurrence, $M_{23}C_6$ particles precipitated predominantly at grain boundaries, causing an earlier onset of abnormal grain growth as compared to samples in which precipitation occurred in the interior of the grains (at lowest temperature, 1090 °C). This effect is associated to the stability and kinetics of dissolution of $M_{23}C_6$ particles;
- The initiation and the kinetics of abnormal grain growth can be predicted by analysing both the thermodynamics and kinetics of second-phase particle dissolution.

Acknowledgements

The authors are grateful to the agencies CNPq - Conselho Nacional de Desenvolvimento Científico e Tecnológico and FAPESP for sponsoring this work.

References

1. Byrne, J.G. Recovery, *Recrystallization and Grain Growth*, The Macmillan Company, New York, p. 93 and p. 106, 1965.

Table 3. Comparison between the dissolution times of $(Ti_{0.92}Mo_{0.08})C$ particles and the onset of abnormal grain growth.

Temperature (°C)	Solution time (min)	Onset of Abnormal Grain Growth (min)
1090	60.5	≈ 125
1110	43.9	≈ 10
1130	32.2	≈ 10
1150	23.8	≈ 5
1200	11.6	≈ 5
1250	5.9	< 5
1300	3.1	< 5

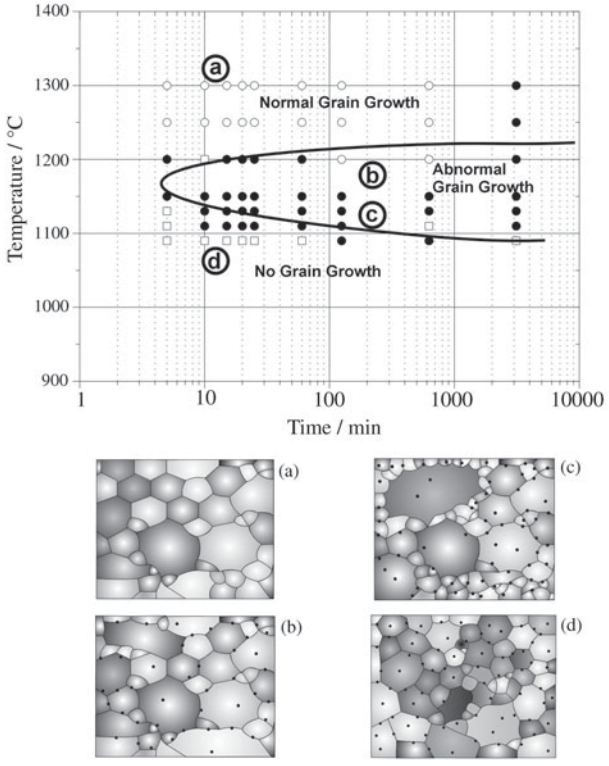

Figure 3. Grain growth map of the samples of this work. Three distinct behaviours can be seen: normal grain growth inhibition (□), abnormal grain growth (●) and normal grain growth (○).

2. Cotterril, P.; Mould, P.R. *Recrystallization and Grain Growth in Metals*, Surrey University Press, London, p. 266, 1976.
3. Detert, K. *Recrystallization of Metallic Materials*, 2nd ed., Dr. Riedrer-Verlag GmbH, Stuttgart (F. Haessner, ed.), p. 97, 1978.
4. Humphreys, F.J.; Hatherly, M. *Recrystallization and Re-*

lated Annealing Phenomena, Pergamon, Oxford, p. 314, 1996.
5. Padilha, A.F.; Siciliano Jr., F. *Encruamento, Recristalização, Crescimento de Grão e Textura*, 2nd ed., ABM, São Paulo, p. 48, 1996.
6. Dutra, J.C. Ph.D. *Thesis*. University of São Paulo, São Paulo. 163p., 1997.
7. Bell, F.C.; Sonon, D.E. *Metallography.* v. 9, p. 91, 1976.
8. Burke, K.E. *Metallography.* v. 8, p. 473, 1975.
9. Padilha, A.F.; Schanz, G.; Anderko, K. *J. Nucl. Mater.*, v. 105, p. 77, 1982.
10. Padilha, A.F. Dr.-Ing. *Thesis.* Fakultät für Maschinenbau der Universität Karlsruhe., 123p., 1981.
11. Deighton, M. *Journal of the Iron and Steel Institute*, v. 208, p. 1012, 1970.
12. Aaron, H.B.; Kotler, G.K. *Metallurgical Transactions.* v. 2, p. 393, 1971.
13. Aaron, H.B. *Metal Science Journal.* v. 2, p. 192, 1968.
14. Whelan, M.J. *Metals Science Journal.* v. 3, p. 95, 1969.
15. Padilha, A.F.; Guedes, L.C. *Aços Inoxidáveis Austeníticos - Microestrutura e Propriedades.* São Paulo, Hemus Editora Ltda., p. 77, 1994.